

NASA MEMO 10-1-58E

**CASE FILE
COPY**

NASA

31-182

MEMORANDUM

TURBULENT HEAT-TRANSFER COEFFICIENTS IN THE
VICINITY OF SURFACE PROTUBERANCES

By Richard J. Wisniewski

Lewis Research Center
Cleveland, Ohio

**NATIONAL AERONAUTICS AND
SPACE ADMINISTRATION**

WASHINGTON

October 1958

4

5

6

7

8

9

NATIONAL AERONAUTICS AND SPACE ADMINISTRATION

NASA MEMO 10-1-58E

TURBULENT HEAT-TRANSFER COEFFICIENTS IN THE
VICINITY OF SURFACE PROTUBERANCES

By Richard J. Wisniewski

SUMMARY

Local turbulent heating rates were obtained in the vicinity of surface protuberances mounted on the cylinder section of a cone cylinder model at a Mach number of 3.12. Data were obtained at Reynolds number per foot of 4.5 and 8 million for an unswept cylinder, a 45° swept cylinder, a 45° elbow, and several 90° elbows.

The unswept cylinder and the 90° elbows increased the local turbulent heating rates in the vicinity of the surface protuberances. The data of the 45° swept cylinder and the 45° elbow resulted in heating rates lower than those observed without surface protuberances. In general, sweeping a surface protuberance resulted in heating rates comparable or lower than those measured without surface protuberances.

INTRODUCTION

The design of high-speed vehicles requires a knowledge of the aerodynamic heating that will be encountered. In most cases maximum local heating rates will occur in the vicinity of the leading edge. However, the possibility of local hot spots at wing or control-surface body junctions and other types of surface protuberances necessitates studies of these shapes. For example, recent experimental studies presented in reference 1 revealed heating rates in the immediate vicinity of a cylindrical protuberance that are four to five times greater than those that would exist without a protuberance.

The present investigation determined to what extent the heat-transfer rate in the vicinity of a surface protuberance would be altered by sweep and other basic modifications. This investigation is limited to a few specific protuberance configurations and is not intended to be of a comprehensive nature.

CF-1

SYMBOLS

c_p	specific heat at constant pressure
h	local heat-transfer coefficient
k	thermal conductivity
q	local heat-transfer rate per unit area
Re	unit Reynolds number, $\frac{u_\infty}{\nu_\infty}$, ft^{-1}
Re_x	length Reynolds number, $\frac{u_\infty}{\nu_\infty} x$
r	body radius
St	undisturbed Stanton number
St'	disturbed Stanton number
T	temperature
t	time
u	velocity
x	axial distance
η	recovery factor, $\frac{T_{aw} - T_\infty}{T_0 - T_\infty}$
θ	meridian angle
ν	kinematic viscosity
ρ	density
τ	wall thickness

Subscripts:

aw	adiabatic wall
b	model material

- w model wall
- ∞ free-stream static conditions ahead of the shock
- 0 stagnation value

APPARATUS AND PROCEDURE

The investigation was conducted at the Lewis laboratory in the 1-by 1-foot supersonic wind tunnel which operates at a Mach number of 3.12. Tests were made at free-stream Reynolds numbers per foot of 4.5 and 8.0 million. The stagnation temperature of the inlet air was approximately 65° F and the tunnel stagnation dew point was -35° F. Further details concerning the facility may be found in reference 2.

The dimensions and instrumentation locations of the 20° cone-cylinder test body are shown in figure 1. The dimensions of the five protuberance shapes tested are given in figure 2. The model was fabricated from monel with a wall thickness of 0.050 inch. Model installation in the tunnel was the same as described in reference 2. The conical portion of the model was sandblasted for a majority of tests in order to insure turbulent flow in the vicinity of the protuberance. In these tests transition occurred between 2 and 4 inches from the leading edge of the test model. In one of the tests reported herein the model was not sandblasted and transition occurred at approximately 6 to 8 inches from the leading edge.

The protuberances were mounted on the cylinder portion of the model, that is, 14 inches back from the leading edge. The method of mounting the protuberances is shown in figure 3. All the protuberances tested were fabricated from plastic.

Precooling the model was accomplished by enclosing the model (protuberances included) in a set of shoes, similar to those used in reference 2, and by passing liquid nitrogen into the shoes and over the model. When the desired wall temperature was obtained (-340° F), the shoes were removed and transient temperature measurements were obtained on a multiple-channel recording oscillograph. A description of the transient technique can be found in reference 2 in greater detail.

DATA REDUCTION

The general equation describing the transient heat transfer to the thin skin cylindrical portion of the model is

$$q_{\text{total}} = q_{\text{convection}} + q_{\text{conduction along the skin}} + q_{\text{radiation}} + q_{\text{conduction to the inside of the model}}$$

or

$$\tau(\rho c_p)_b \frac{\partial T_w}{\partial t} = h(T_{aw} - T_w) + \left(\frac{\tau k_b}{r^2} \frac{\partial^2 T_w}{\partial \theta^2} + k_b \tau \frac{\partial^2 T_w}{\partial x^2} \right) + q_{\text{radiation}} + q_{\text{conduction to inside of model}} \quad (1)$$

The magnitude of the radiation and conduction terms in equation (1) was less than 2 percent for tests in which the model was free of protuberances and also in the tests of the 45° elbows and swept-cylinder protuberances. However, in the tests of the cylinder protuberances and the

90°-elbow protuberances, the axial conduction term $k_b \tau \frac{\partial^2 T_w}{\partial x^2}$ was large

enough to underestimate the total heat input by as much as 15 percent. The axial conduction error was determined by numerically taking the second derivative of a curve faired through the experimental temperature distribution. A typical axial temperature distribution for a cylinder protuberance is shown in figure 4(a). Since there is a reasonable amount of uncertainty present in the proper fairing of the temperature distribution data, no attempt was made to correct the data for conduction errors. Therefore, in calculating the local heat-transfer coefficients the following expression was used for all the data

$$h = \frac{\tau(\rho c_p)_b \frac{dT_w}{dt}}{T_{aw} - T_w} \quad (2)$$

The time rate of change of the temperature was found from temperature-time curves faired by the method of least squares and differentiated numerically using a five-point method. Fitting of the data by the method of least squares and numerical differentiation was accomplished with an IBM 650 computer.

The adiabatic wall temperature T_{aw} was usually obtained from the following equation using experimentally determined recovery factors

$$T_{aw} = T_\infty + \eta(T_0 - T_\infty) \quad (3)$$

A typical distribution of the experimental recovery factor in the vicinity of a cylinder protuberance is shown in figure 4(b). In some instances, however, experimental recovery factors were not available. In these cases the adiabatic wall temperatures were obtained in the following

manner. Temperature data were plotted against the reciprocal of time and extrapolated to the point where $1/t = 0$. The temperature calculated in this manner was considered the adiabatic wall temperature. In all cases this extrapolation was a straight line parallel to the inverse time axis, because temperature-time histories were available close to adiabatic wall conditions.

Evaluation of the heat-transfer coefficient requires a knowledge of the variation of specific heat of the model material with temperature. The specific heat of monel has been measured over the temperature range of this investigation in reference 3.

When the experimental values of the local heat-transfer coefficient were determined, the corresponding values of free-stream Stanton numbers were computed from the following expression

$$St = \frac{h}{\rho_{\infty} u_{\infty} c_{p, \infty}} \quad (4)$$

The accuracy of the experimental Stanton numbers was estimated to be ± 16 percent for the clean model, the 45° -swept-cylinder and 45° -elbow protuberances. Since the conduction error is important for the cylinder and 90° -elbow protuberances, the relative error of the Stanton number in these cases becomes $+16$ and -31 percent. However, since a Stanton number ratio is presented, the error in this ratio should be less than $+16$ and -31 percent.

As in reference 4 the model was subjected to two condensation films. However, the calculations of reference 4 indicate that condensation did not have an appreciable effect on the determination of heat-transfer coefficients.

RESULTS AND DISCUSSION

Experimental turbulent Stanton numbers are presented in figure 5 for the model without protuberances at an average wall-to-free-stream temperature ratio of 1.5 and free-stream Reynolds numbers per foot (Re_{∞}) of 4.5 and 8 million. For both Reynolds number conditions, transition was fixed between 2 and 4 inches on the cone by sandblasting the conical portion of the model. Also included in figure 5 is the turbulent flat-plate theory of reference 5 at a wall-to-free-stream temperature ratio of 1.5. Free-stream conditions were used to obtain the theoretical flat-plate Stanton numbers since the local conditions on the cylinder are approximately those of the free stream.

The data presented in figure 5 represent the undisturbed Stanton numbers St_{∞} . These data are compared with the measured Stanton numbers

in the vicinity of the various tested surface protuberances in figures 6 to 7. In order to determine the effect of the protuberance ratio of the disturbed to undisturbed Stanton number, St'_{∞}/St_{∞} is formed, and in order to decrease the scatter in the Stanton number comparison, a least square fit of the undisturbed Stanton number data was used.

The ratio of the disturbed to the undisturbed Stanton number St'_{∞}/St_{∞} for a cylinder protuberance (shape A) is plotted in figure 6. Since the position of transition may influence the heat-transfer measurements in the vicinity of the protuberance, transition was fixed between 2 and 4 inches on the cone. Fixing transition on the cone yielded well established turbulent flow at the protuberance and eliminated the length of turbulent run as a variable in the tests. In subsequent measurements discussed later, transition was also fixed on the cone unless otherwise stated.

In figure 6(a) the values of St'_{∞}/St_{∞} are presented for a Reynolds number per foot of 8 million. The largest values of St'_{∞}/St_{∞} , approximately 1.5 to 1.7, were measured in the vicinity of the protuberance on the 0° and 22.5° generator. The limited results obtained on the 45° generator show no appreciable rise over the undisturbed Stanton number value. In order to investigate a possible Reynolds number effect, data were obtained at a Re_{∞} of 4.5 million per foot. These results are plotted in figure 6(b). With the exception of a few points these data are quite similar to those of figure 6(a). It appears that there is no Reynolds number effect over the Reynolds number per foot range investigated. Similar results, not presented here, were also obtained for all other protuberances tested.

The effect of sweeping the cylinder to 45° is presented in figure 6(c). These data are for protuberance shape B at a Re_{∞} of 8 million per foot. Sweeping the protuberance yields values of 0.7 to 1.0 for St'_{∞}/St_{∞} on the 0° and 22.5° generators. The values of St'_{∞}/St_{∞} on the 45° generator are 0.6 to 0.7. Thus, the 45° swept cylinder yields values of St'_{∞}/St_{∞} 40 to 50 percent lower than the heat transfer measured in the vicinity of an unswept protuberance. Furthermore, the swept cylinder heat-transfer measurements are lower than the undisturbed heating rates.

Presented in figure 6(d) are data obtained with the 90° -elbow protuberance at a Re_{∞} of 8 million per foot. This protuberance is of the same diameter and height as the unswept cylinder protuberance. As in the case of the cylinder protuberance, figure 6(a), the heating rates in the vicinity of the 90° elbow are greater than the undisturbed heating rates. However, the largest values of St'_{∞}/St_{∞} are definitely less than those for the cylinder of figure 6(a). In fact, the values of St'_{∞}/St_{∞} on the 45° generator in the vicinity of the 90° elbow are less than the undisturbed heating rates.

A difference in the Stanton number ratio upstream of the two protuberances is noted in comparing figures 6(a) and (b). Although these protuberances are of the same height and diameter, the difference in the downstream shape of the protuberance must alter the subsonic flow field sufficiently upstream to change the heating rates ahead of the protuberance. Thus, the heating rates ahead of protuberance C are appreciably less than those ahead of protuberance A.

The data for the 45° elbow are presented in figure 6(e). A comparison of figure 6(e) with figure 6(c) reveals that the heating rates measured in the vicinity of the 45° swept cylinder and the 45° elbow are similar. Values of St_w'/St_w of 0.6 to 1.0 are obtained. The data measured on the 45° generator are again lower than the undisturbed values.

The effect of protuberance diameter and height on the heat transfer in the vicinity of the protuberance is of considerable interest. Data obtained in the vicinity of two 90° elbows are presented in figure 7. Since the conical portion of the model was not sandblasted for shape D, transition from laminar to turbulent flow occurred at approximately 6 to 8 inches from the leading edge of the model.

Protuberance shape D had a diameter of 0.498 inch and a height of 0.598. The data of protuberance C, presented in figure 6(d), are also included here for comparison purposes. Shape C had a diameter of 0.345 inch and a height of 0.441 inch. The effect of protuberance size on the local heating rates for this study can be obtained by examining the data of figure 7. This comparison indicates that the larger protuberance had the greatest effect on the local heating rates.

Another effect which would be of considerable interest but has not been examined here is the effect of mounting the protuberances on a flat plate rather than on a cylinder. It is probable that the heat-transfer measurements presented here would differ from those found on a flat plate with the same protuberances and local conditions. This fact might be especially true for those stations on the plate which would correspond to the 22.5° and 45° generators of the cylinder. Of course, a change in the heat transfer would not be too surprising since the flow field in the vicinity of the protuberance would be altered.

SUMMARY OF RESULTS

Heat-transfer measurements made in the vicinity of surface protuberances yield the following results:

1. Unswept cylindrical surface protuberances can increase the local heating rates in the vicinity of the protuberance by as much as 70 percent over the undisturbed heating rates.

2. Sweeping cylindrical surface protuberances by 45° resulted in local heating rates in the vicinity of the protuberance slightly lower than the undisturbed rates.

3. Local heating rates measured in the vicinity of 45° and 90° elbows did not increase over those measured in the vicinity of 45° and 90° cylinders.

4. In some cases, heating rates measured on the 45° generator were as much as 40 percent lower than those observed without protuberances.

Lewis Research Center

National Aeronautics and Space Administration
Cleveland, Ohio, July 15, 1958

REFERENCES

1. Bloom, Martin H., and Pallone, Adrian: Heat Transfer to Surfaces in the Neighborhood of Protuberances in Hypersonic Flow. Preprints from Heat Transfer and Fluid Mech. Inst. (Pasadena), June 19-21, 1957, pp. 249-278.
2. Jack, John R., and Diaconis, N. S.: Variation of Boundary-Layer Transition with Heat Transfer on Two Bodies of Revolution at a Mach Number of 3.12. NACA TN 3562, 1955.
3. Hampton, W. F., and Mennie, J. H.: The Specific Heat of Monel Metal Between -183° and 25° C. Canadian Jour. Res., vol. 7, July-Dec. 1932, pp. 677-678; discussion, pp. 678-679.
4. Jack, John R., and Diaconis, N. S.: Heat-Transfer Measurements on Two Bodies of Revolution at a Mach Number of 3.12. NACA TN 3776, 1956.
5. Lee, Dorothy B., and Faget, Maxime A.: Charts Adapted from Van Driest's Turbulent Flat-Plate Theory for Determining Values of Turbulent Aerodynamic Friction and Heat-Transfer Coefficients. NACA TN 3811, 1956.

Thermocouple locations

Axial distance, in.	2.00	4.00	6.50	8.50	10.50	12.50	12.875	13.125	13.375	13.625	14.00	14.375	14.625	14.875	15.125	15.50	16.50
0° Generator	1	2	3	4	5	6	7	8	9	10	Protuberance	11	12	13	14	15	16
22.5° Generator								17	18	19	20	21	22	23	24	25	
45° Generator											26	27	28	29	30	31	

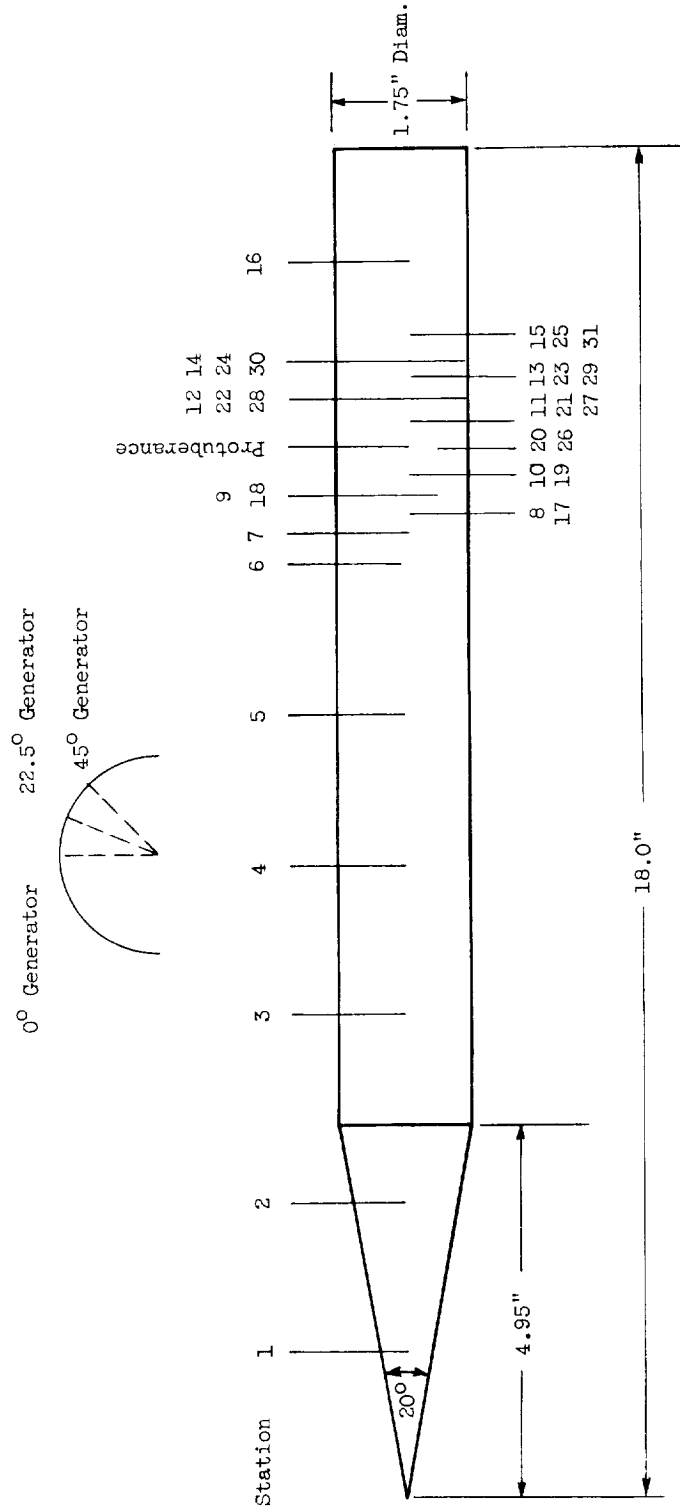
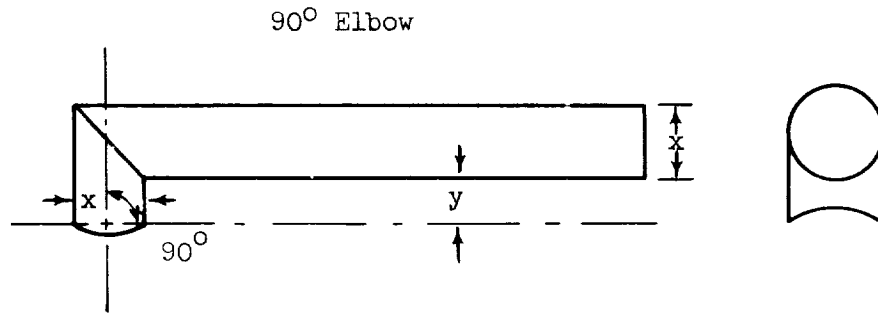
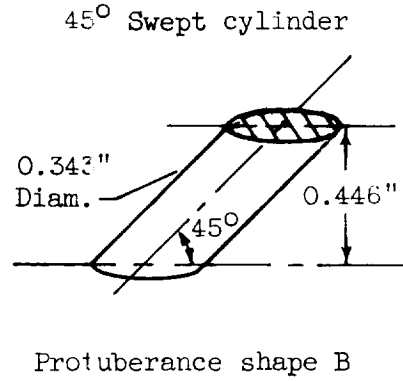
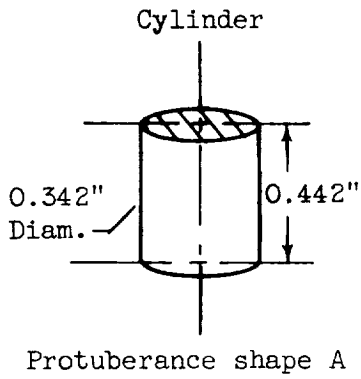
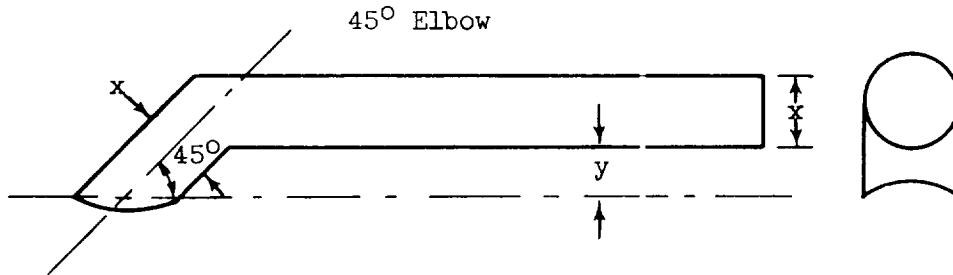


Figure 1. - Model details and thermocouple locations.



Protuberance shape	x, in.	y, in.	Angle
C	0.345	0.096	90°
D	0.498	0.091	90°



Protuberance shape	x, in.	y, in.	Angle
E	0.342	0.090	45°

Figure 2. - Protuberance shapes tested.

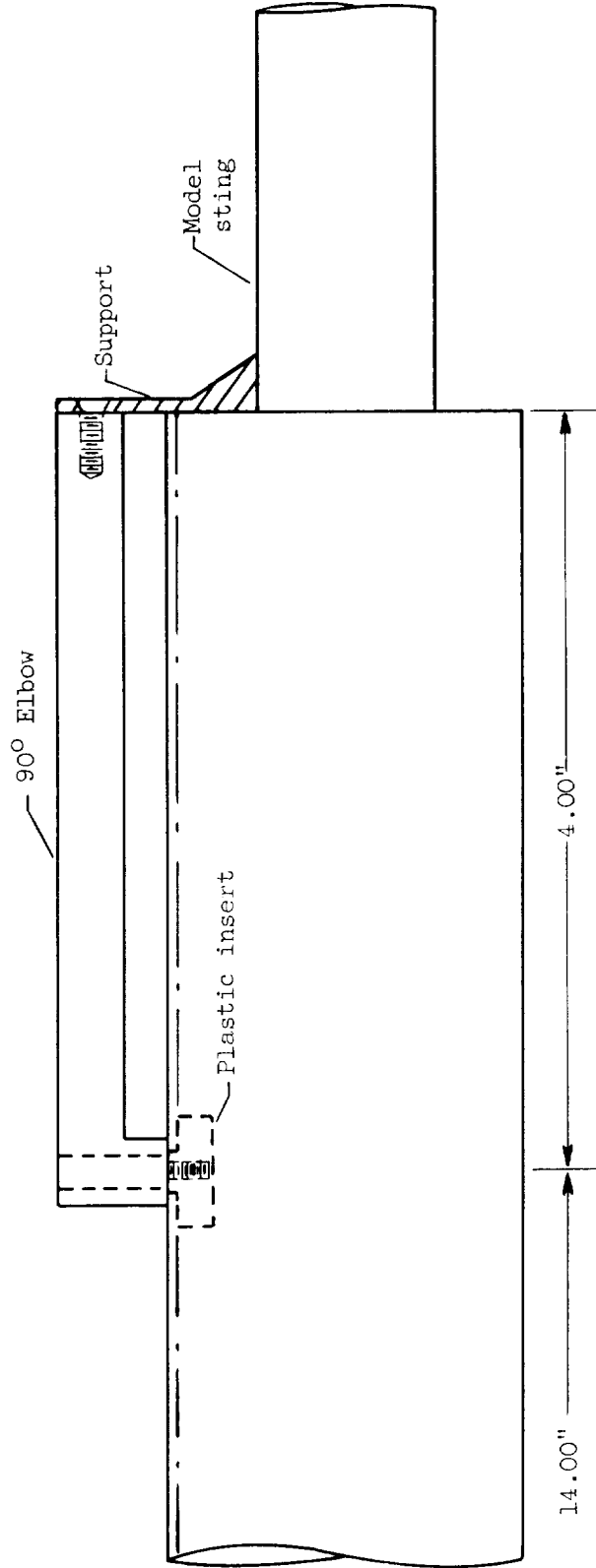
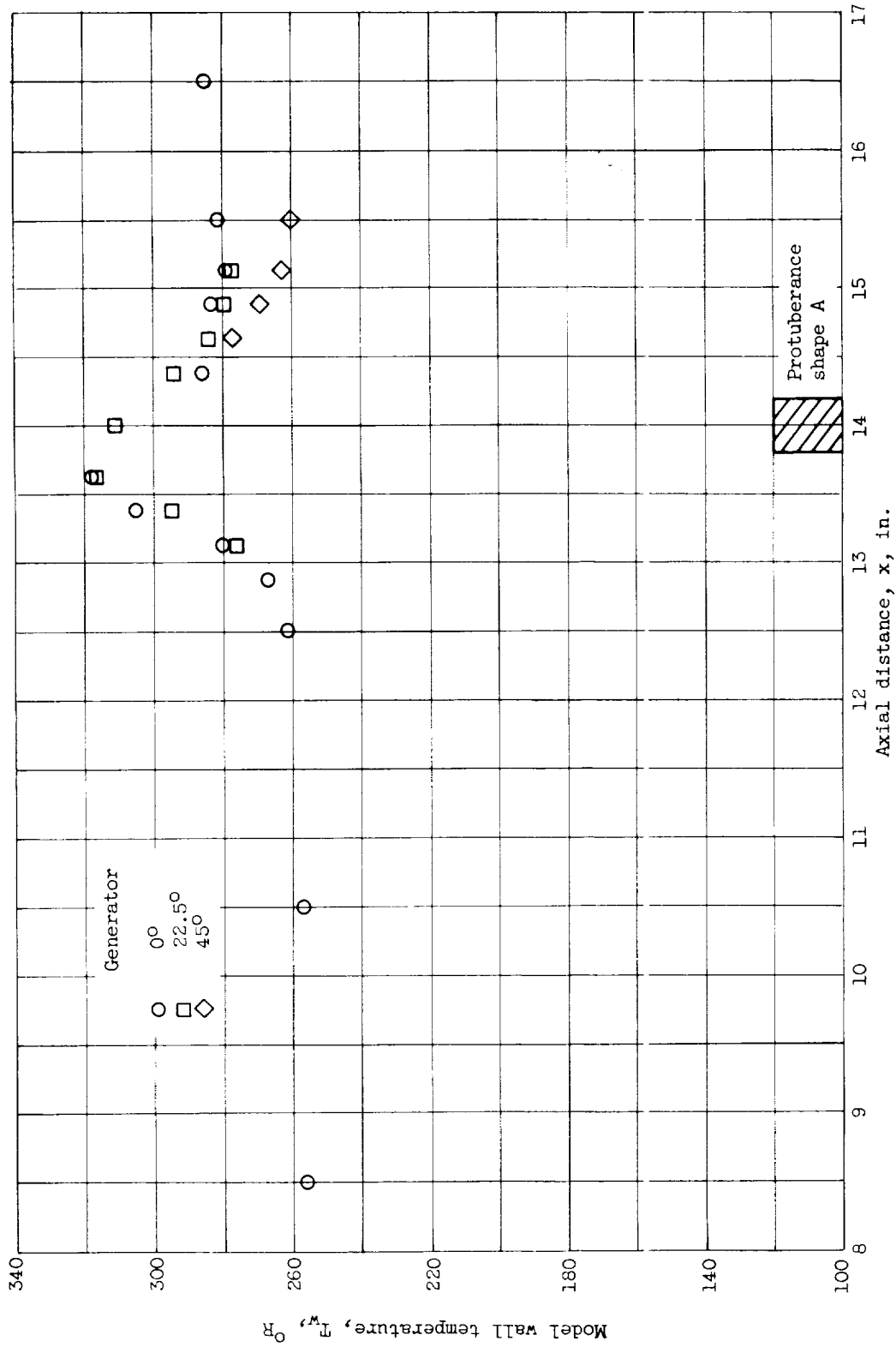
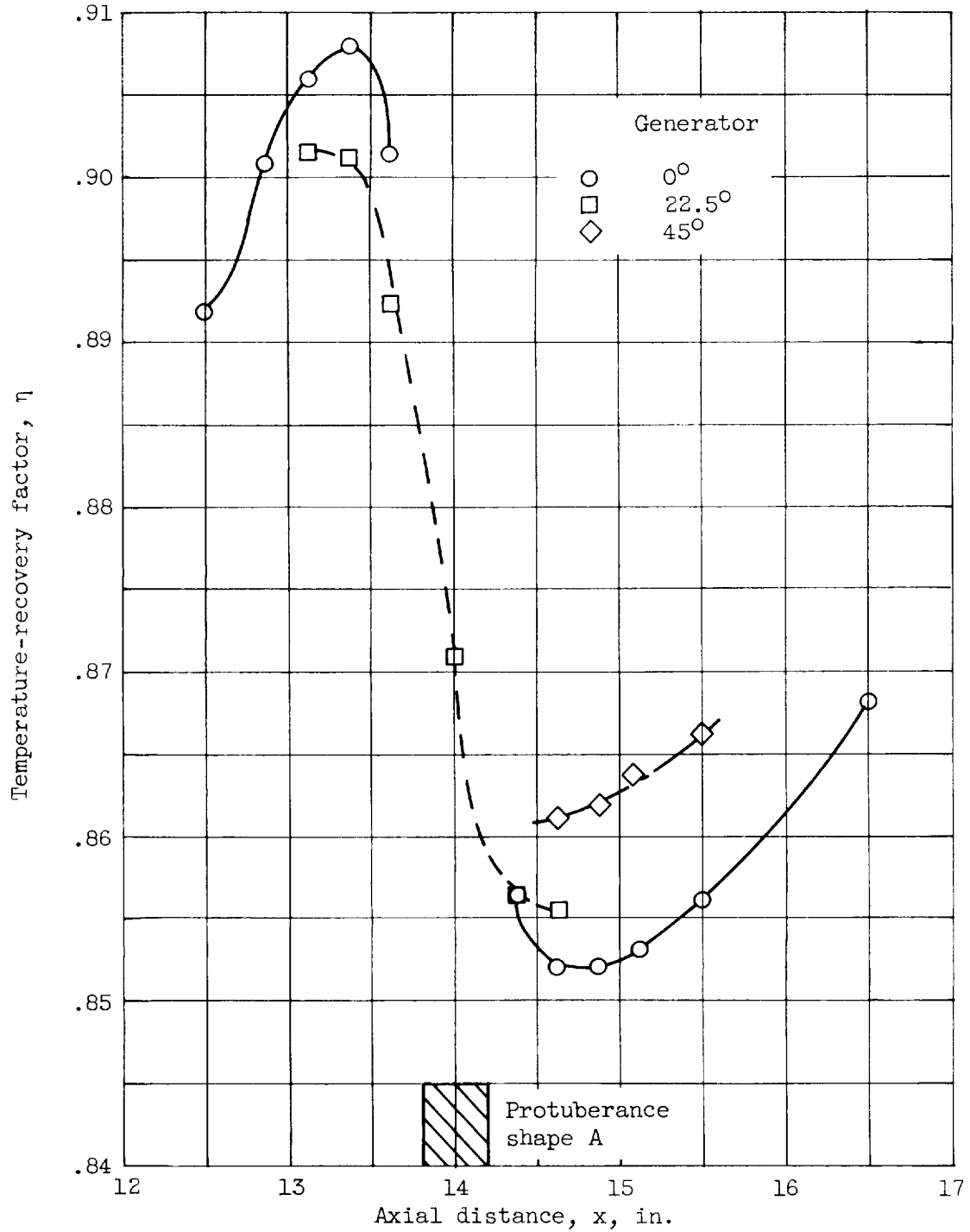


Figure 3. - Details of protuberance installation.



(a) Surface-temperature distribution.
 Figure 4. - Typical distributions in the vicinity of a 90° protuberance.



(b) Recovery-factor distribution

Figure 4. - Concluded. Typical distributions in the vicinity of a 90° protuberance.

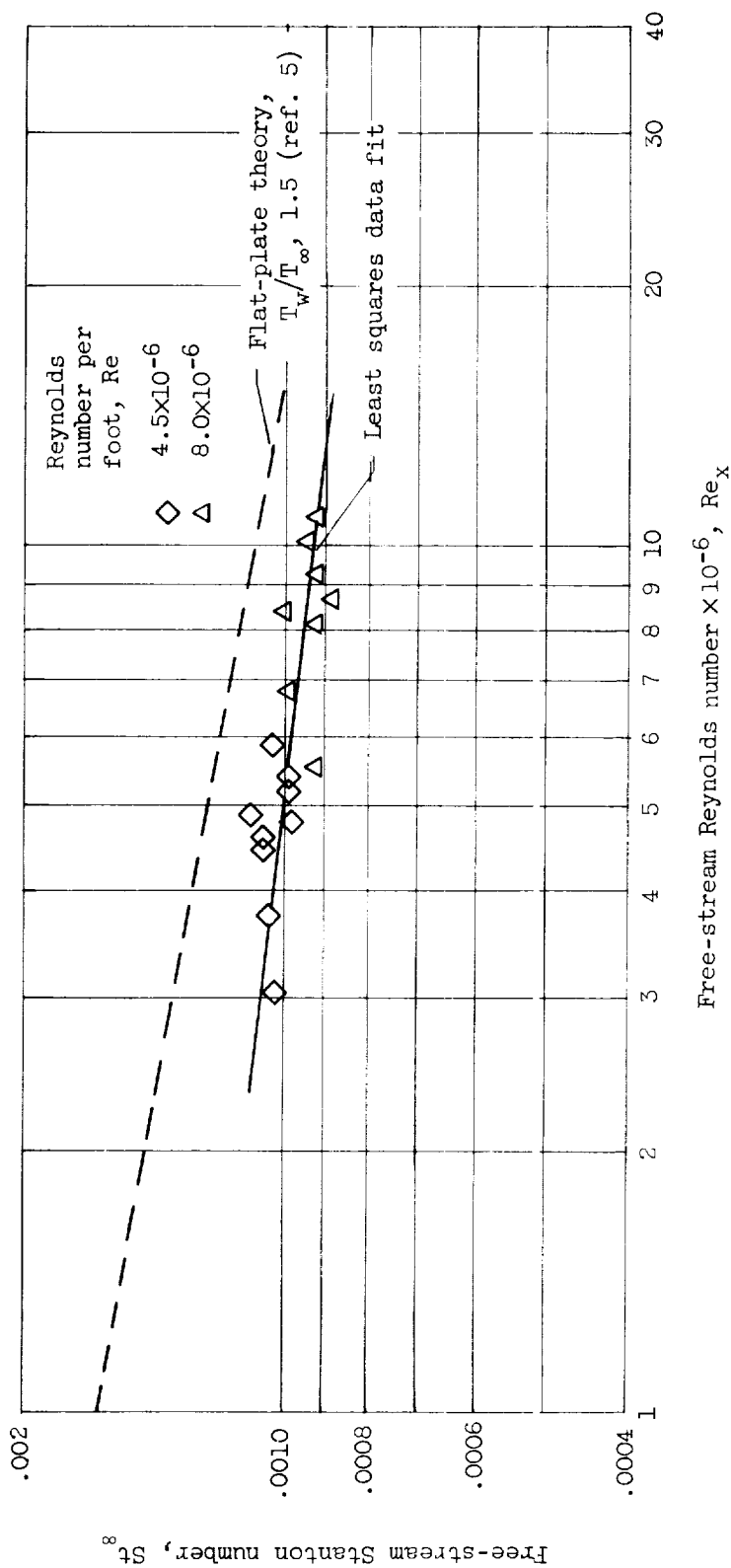
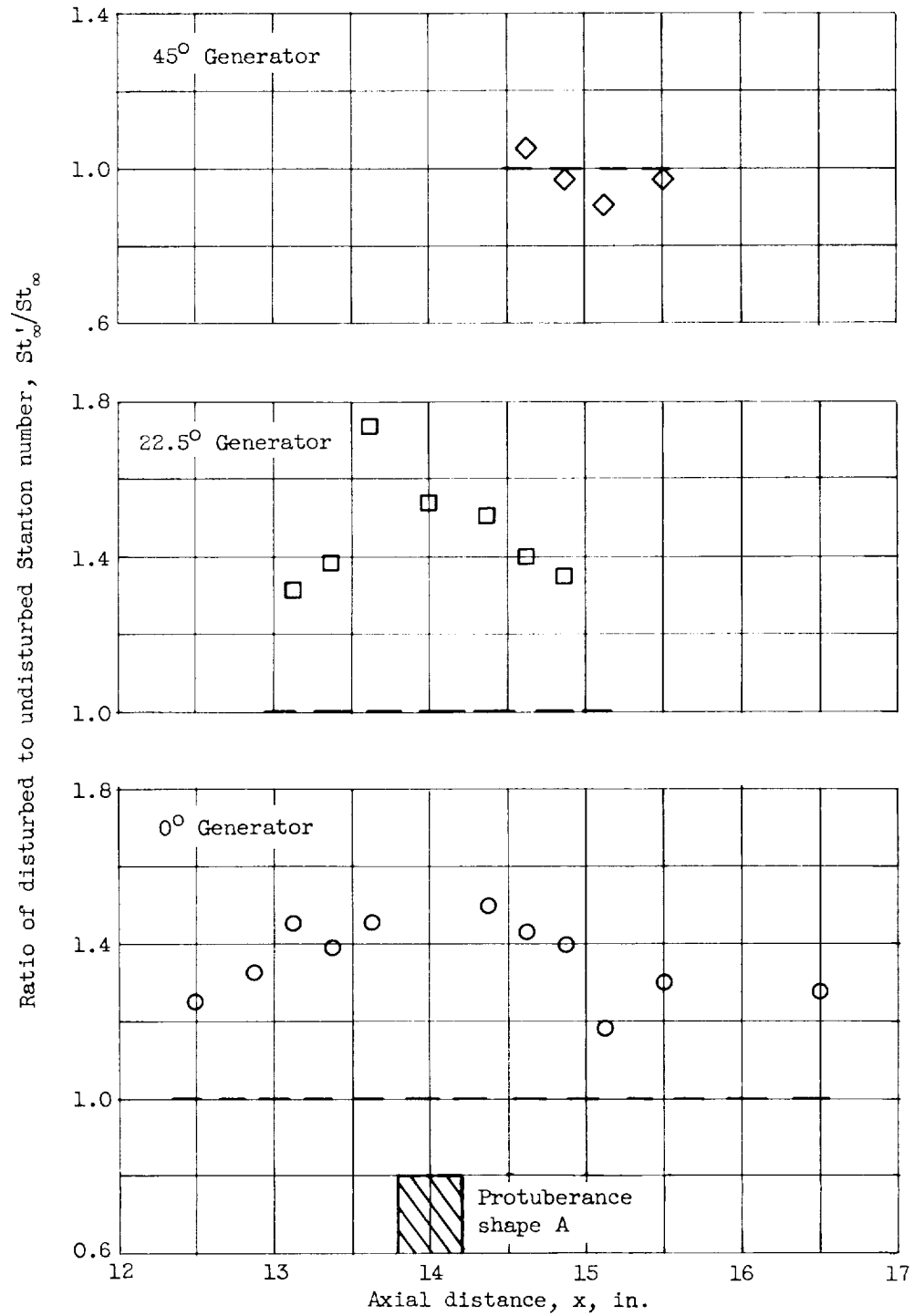
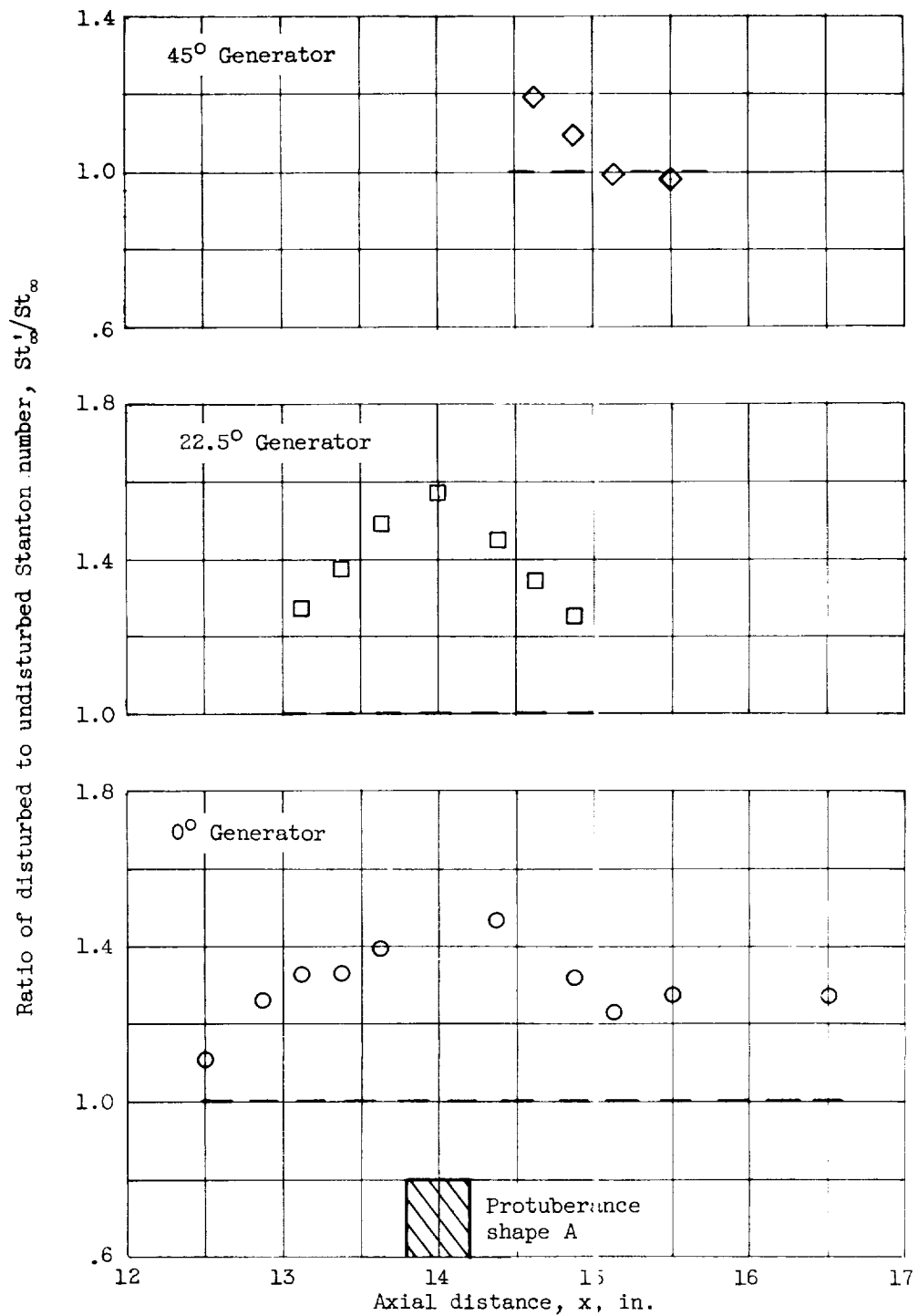


Figure 5. - Undisturbed local turbulent heat-transfer coefficients.



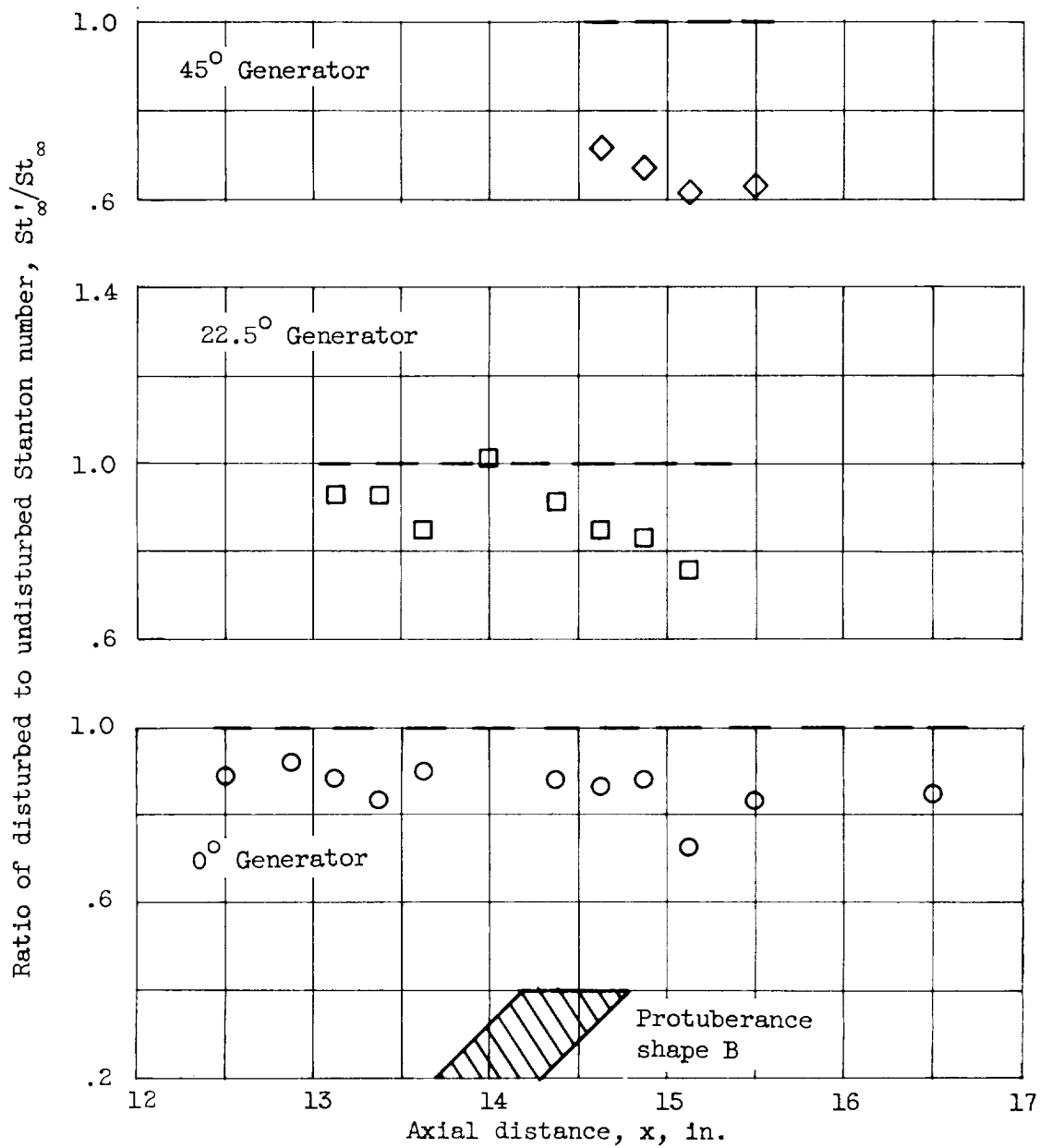
(a) Cylinder protuberance; Reynolds number per foot of 8×10^6 .

Figure 6. - Local turbulent heat-transfer coefficients in the vicinity of a protuberance.



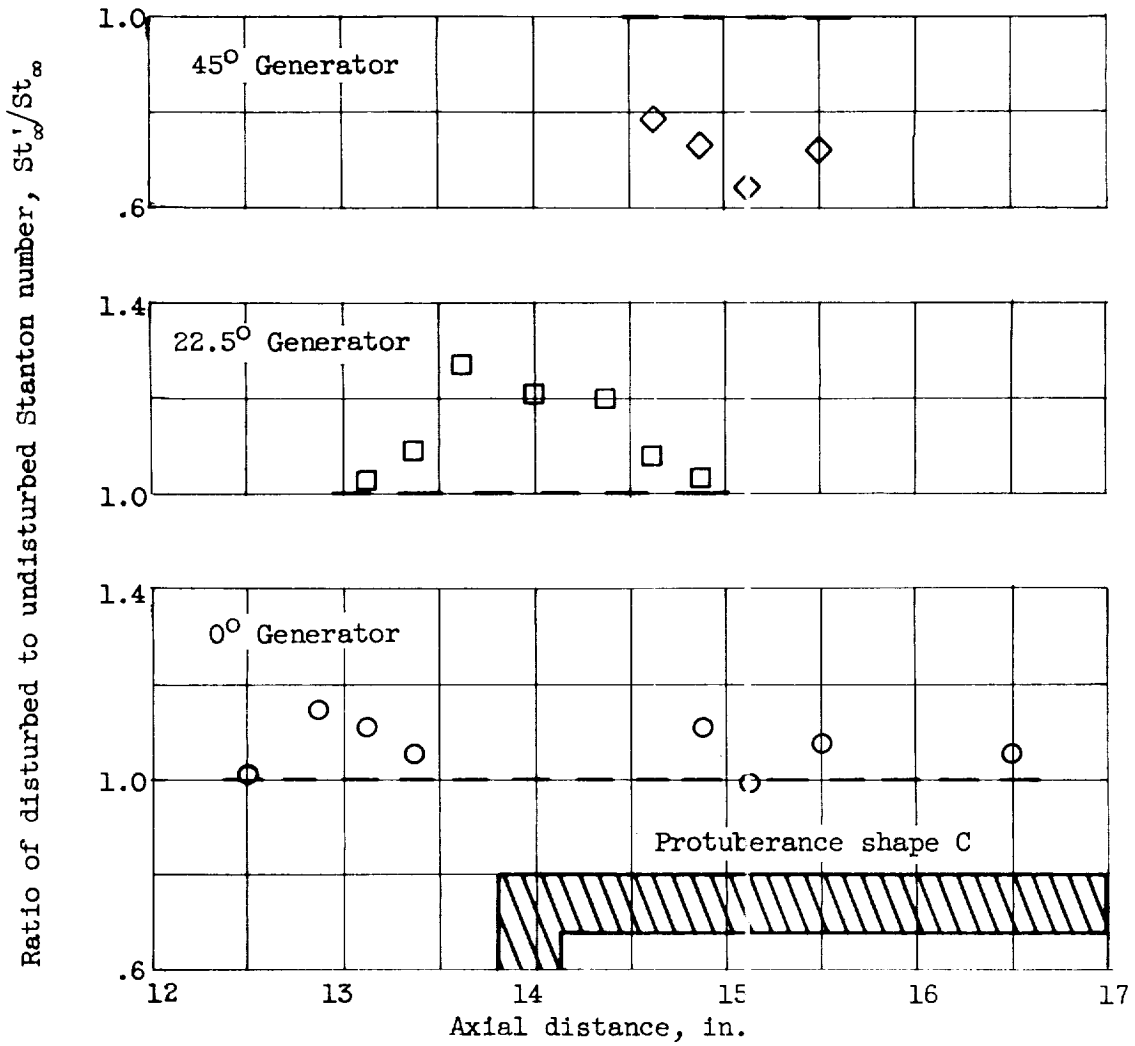
(b) Cylinder protuberance; Reynolds number per foot of 4.5×10^6 .

Figure 6. - Continued. Local turbulent heat-transfer coefficients in the vicinity of a protuberance.



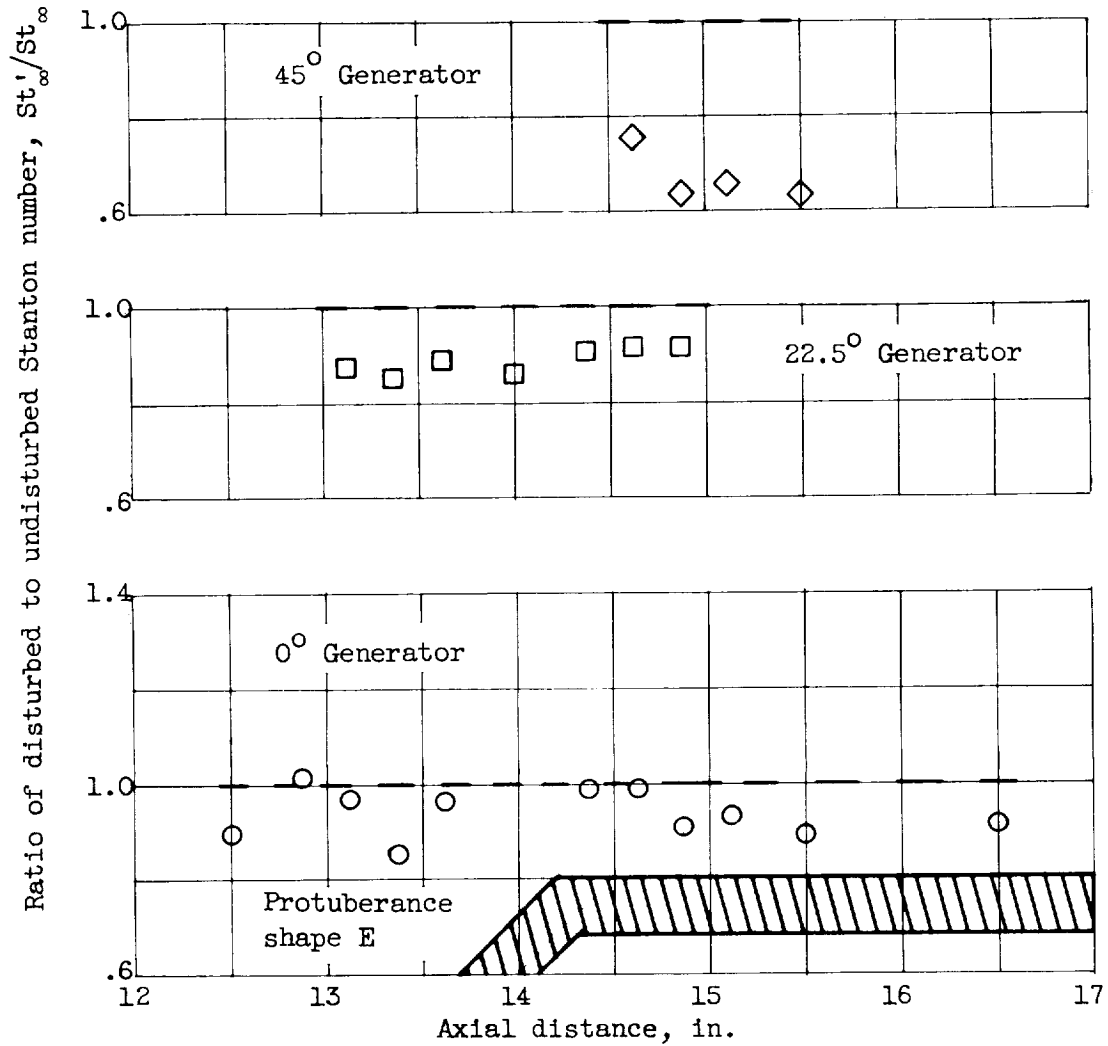
(c) 45°-Swept-cylinder protuberance; Reynolds number per foot of 8×10^6 .

Figure 6. - Continued. Local turbulent heat-transfer coefficients in the vicinity of a protuberance.



(d) 90°-Elbow protuberance; Reynolds number per foot of 8×10^6 .

Figure 6. - Continued. Local turbulent heat-transfer coefficients in the vicinity of a protuberance.



(e) 45°-Elbow protuberance; Reynolds number per foot of 8×10^6 .

Figure 6. - Concluded. Local turbulent heat-transfer coefficients in the vicinity of a protuberance.

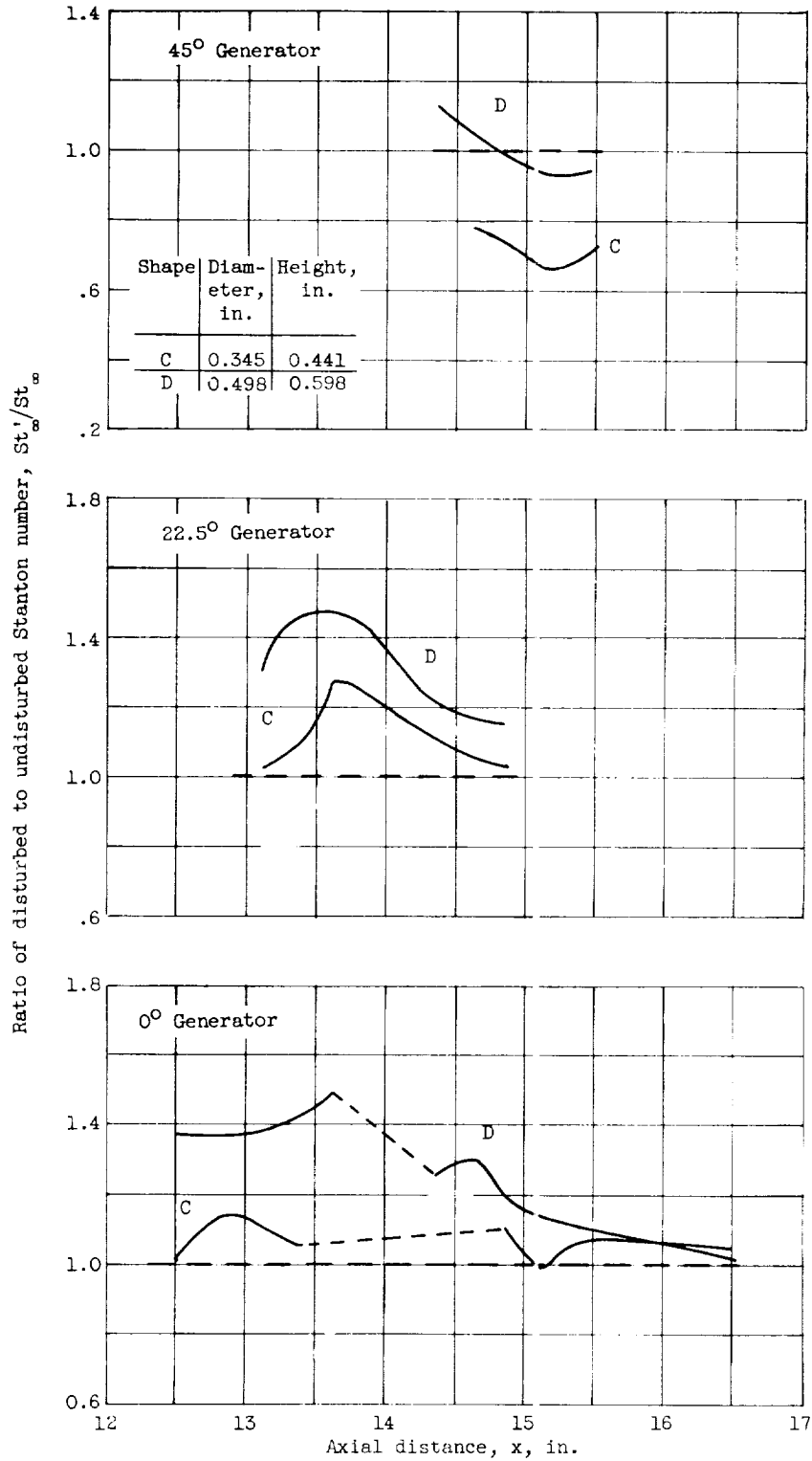


Figure 7. - Effect of protuberance size on the local heating rates in the vicinity of 90° elbows; Reynolds number per foot of 8×10^6 .